Journal of Physics D: Applied Physics

PAPER • OPEN ACCESS

Mitigating dust particle contamination in an afterglow plasma by controlled lifting with a DC electric field

To cite this article: Neeraj Chaubey and J Goree 2024 *J. Phys. D: Appl. Phys.* **57** 105201

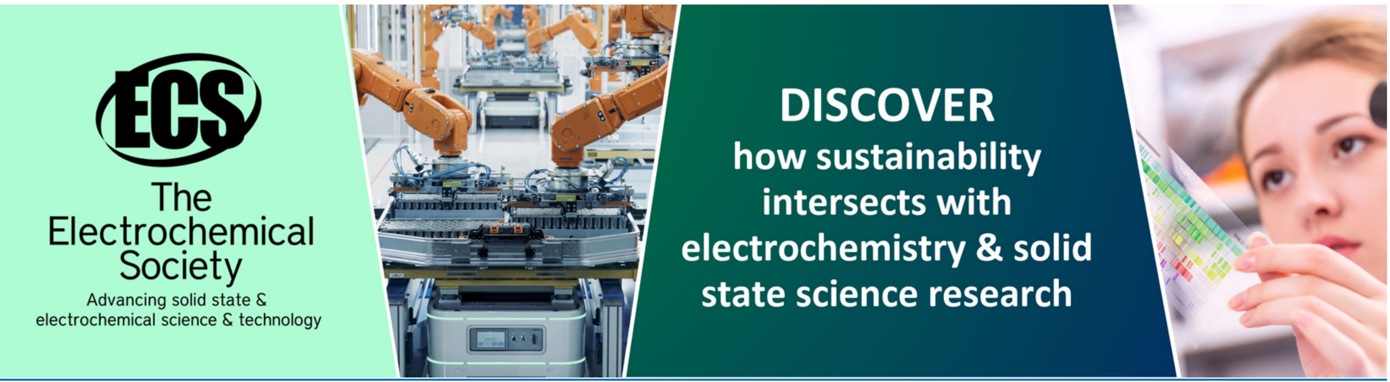

OPEN ACCESS
IOP Publishing

Journal of Physics D: Applied Physics

J. Phys. D: Appl. Phys. **57** (2024) 105201 (6pp)

https://doi.org/10.1088/1361-6463/ad1148

Mitigating dust particle contamination in an afterglow plasma by controlled lifting with a DC electric field

Neeraj Chaubey* **and J Goree**

Department of Physics and Astronomy, University of Iowa, Iowa City, IA 52242, United States of America

E-mail: neeraj-chaubey@uiowa.edu

Received 7 September 2023, revised 20 November 2023
Accepted for publication 30 November 2023
Published 8 December 2023

Abstract

Particle contamination due to plasma processing motivates the design of a method of electrically lifting particles in a time interval after a plasma's power is turned off. Small solid dust particles have electric charges that are not frozen until a late stage of the plasma afterglow. Beyond that time, before they fall to a surface below and cause defects, particles can be lifted in a controlled manner by applying an appropriate direct-current (DC) electric field, as we demonstrate experimentally. A few milliseconds after an argon plasma's capacitively coupled radio-frequency power is switched off, a vertical DC electric field is applied. Thereafter, video imaging shows that the falling of the particles is slowed or stopped altogether, depending on the magnitude of the upward electric force.

Keywords: dusty plasma, afterglow plasma, particle contamination control

1. Introduction

Small solid particles can cause defects in semiconductor wafers, reticles, and other substrates. These particles can develop not only during handling at one atmosphere, but also under vacuum conditions during plasma processing, either by condensing in the gas phase or by flaking of films from surfaces [1].

It has been known at least since 1989 that micron-size and smaller particles can be electrically levitated in a processing plasma [2]. A particle gains an electric charge Q by collecting unequal positive and negative charges from the plasma, and due to this charge the particle can be levitated by an electric field in the plasma [3–36], for example the direct-current (DC) (i.e. steady-state) electric field that occurs naturally in an electrode sheath above a horizontal lower electrode. When the power that sustains the plasma is turned off, the levitation ceases and particles can fall onto critical surfaces, like wafers and masks, and contaminate them [1, 2, 37].

The crucial time interval, when particles can fall onto a surface, coincides with the plasma afterglow [9, 12–14, 38–72]. Controlling the conditions during this afterglow will be the focus of this paper. We can distinguish two stages of the afterglow, in terms of what happens to the particles. In an *early* stage of the afterglow, generally in the first few milliseconds, enough electrons and ions from the plasma remain in the chamber that they can alter a particle's charge, compared to what it had when the plasma was powered. While the particles were generally negatively charged while the plasma was powered [9–24, 26–35, 73], in the afterglow the particles can become either positively or negatively charged [9, 12–14, 45–71], depending on the afterglow conditions and particularly depending on the presence of DC electric field [74]. Following this early stage of the afterglow when the charge can be altered, most electrons and ions will escape the plasma chamber, leaving too few of them to cause further changes in the particle's charge. At that point, the particle's charge is

* Author to whom any correspondence should be addressed.

said to be frozen [74–77], which marks the beginning of the *late* stage of the afterglow. The duration of the early stage of afterglow charging can be a millisecond or longer, while the late stage lasts until the particle falls to a surface, which can last tens of milliseconds [74, 77]. When the particles do land on the substrate surface, they contaminate it, which can lead to a defect.

Mitigating this contamination can be accomplished by several methods. We have found that the most abundant source of literature for these mitigation methods are patents [78–85], while journal articles mention fewer methods. One of the earliest mentioned mitigation methods involves increasing the gas flow, at the end of a plasma process, so that a gas-drag force purges particles by sweeping them toward a vacuum pump port, thereby removing them from the vicinity of the substrate [1, 2, 78].

In this paper we further develop a contamination mitigation strategy that we suggested recently [76], which we summarize briefly. The mitigation strategy has two steps: charging control and lifting control, which both make use of recent fundamental physics discoveries about the plasma afterglow. *Charging control* would be performed during the early stage of the afterglow while electrons and ions remain in the chamber in sufficient number to change the particle's charge. This change of the charge, during the early stage of the afterglow, was observed in an experiment of Chaubey *et al* [74], who found that a DC electric field plays a key role in determining the value of the frozen charge. *Lifting control*, on the other hand, would generally be performed in the late stage of the afterglow, taking advantage of the frozen charge on a particle.

Here, we will focus on the lifting control. Like charging control, lifting control will depend on factors that include an applied DC electric field. We suggested the possibility of this lifting control in [76], but without data to support that suggestion. Here we provide that supporting data, from a more recent experiment, confirming that particles can be lifted sufficiently to prevent them from falling, by adjusting the electric field during the late stage of the afterglow.

2. Experiment

An experiment was performed using a capacitively coupled radio frequency plasma. High speed imaging was used to measure the height of a particle layer versus time, so that we could identify conditions that slowed or even prevented particles from falling to the surface below.

Many of the experimental conditions were the same as in [76], where our purpose was to study the horizontal expansion of the dust cloud. The conditions that were the same for the present experiment include 8 mTorr Argon gas, which was partially ionized during plasma operation by applying 13 MHz radio-frequency (RF) power with an amplitude of 305 V peak-to-peak. Less than 2 W of power was deposited in the plasma. There was negligible heating of surfaces, as indicated by a surface temperature that was measured to remain unchanged within 0.1 °C when turning the plasma on.

We used the same two electrodes to power the plasma, and then later to control the lifting in the afterglow. One electrode was the chamber wall, which was always grounded. The other was a horizontal lower electrode, which was capacitively coupled to the RF power during the plasma operation. The lower electrode was also connected to a switched DC power supply, for lifting control during the late stage of the afterglow. While the plasma was powered, the lower electrode naturally developed a negative DC self-bias voltage of -150 V. This DC bias remained after switching off the RF power, due to the 50 nF coupling capacitor.

The particles used were 8.69 μm diameter microspheres. They were made of melamine formaldehyde, which avoids coagulation when handling the powder in a dry form. The particle mass was $m = 5.2\times10^{-13}$ kg, based on manufacturer's data [93]. We note that the particle diameter reported by the manufacturer can have systematic errors, reported by other users who used electron microscopes to measure the sizes of particles from different batches but the same manufacturer as ours. These systematic errors in the size of particles, taken directly from the bottles, can be [86, 87] of order 5%. After exposure to argon plasma, even without added oxygen, there can be a further reduction in diameter due to etching [86, 88], although this is probably less than a 1% change for our brief plasma exposure of a few minutes.

About a thousand particles were dropped from the top of the chamber, by agitating a dispenser. As they fell, the particles gained a negative charge, as is typical in a low-temperature plasma [74]. The particles immediately settled in a single horizontal layer in the electrode sheath, due to a balance of gravity and an upward electric force. This electrical levitation of particles persisted as long as the RF power was on.

At $t = 0$, we switched off the RF power, to begin the afterglow conditions. Simultaneously, a side-view video camera was triggered to begin recording at 1000 frames per second. This 12-bit Phantom v5.2 camera was fitted with a 52 mm-focal-length Nikon macro lens to view a cross-section of the particle layer, which was illuminated by a vertical sheet of laser light from a 671 nm diode laser. Each particle that we measured appeared as ten or more contiguous pixels in an image from an individual frames of the video. We analyzed those images using ImageJ [90], which calculated the particle coordinates with sub-pixel accuracy using the measured intensity of each contiguous pixel in the image of a particle.

Initially, the lower electrode retained its -150 V negative DC bias due to the coupling capacitor C_{coupl}. This bias, which we allowed to persist for 2 ms, led to a DC electric field that drove an ion flow that charged the particles positively, during the early stage of the afterglow [74]. The early stage, as we define it here, ends at the freezing time, which is approximately t=1.5 ms under these experimental conditions, based on measurements to determine when the residual charge no longer responded to a time-delayed change in afterglow-plasma conditions [77].

Differently from the experiment in [74], here we reversed the electric field at $t = 2$ ms by switching the bias on the lower

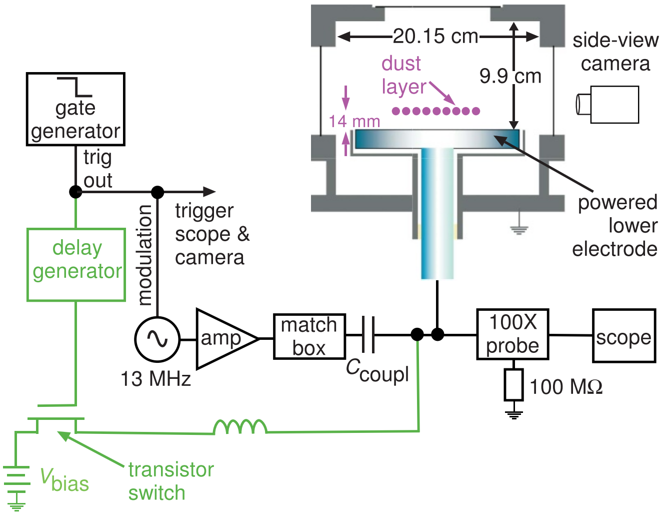

Figure 1. Side-view sketch of the setup. The transistor switch was used here for lifting control during the late stage of the afterglow by applying a DC bias to the lower electrode after a delay of 2 ms, which was long enough that the particle charge was frozen, and ions had largely departed the chamber [74]. For our earlier charging-control experiment [77], we used the same setup but with a delay time <2 ms in order to adjust the electric-field conditions during the early stage of the afterglow, when ions were still present in sufficient number to alter the particle charge. Reproduced from [77].

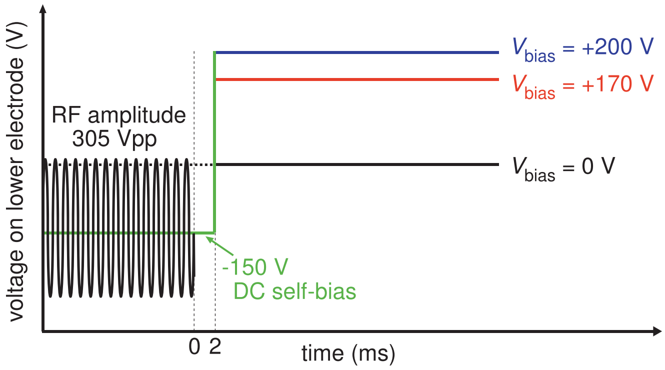

Figure 2. Sketch of the voltage waveform on the lower electrode. An RF voltage of 305 $V_{\rm PP}$ was applied to the lower electrode, which developed a self-bias voltage of -150 V. At $t = 0$, the RF power was turned off, and thereafter the lower electrode maintained its DC self-bias voltage due to the presence of the coupling capacitor $C_{\rm coupl}$. The transistor switch was activated after a delay of $t = 2$ ms to apply a non-negative $V_{\rm bias}$, which was 0 V, +170 V, or +200 V, for three experimental runs.

electrode, using a field-effect transistor shown schematically in figure 1. Since the dust particle charge was already frozen, the electric field that we applied for $t > 2$ ms was intended to provide lifting control rather than charging control. During this late stage of the afterglow, any remaining electrons and ions are assumed to be so rarefied that the electric field is essentially a vacuum field, which can be calculated by solving Laplace's equation as in [74].

We repeated the experiment for several runs, each with a different value of the electric field. For this paper, we report three runs that are particularly instructive. A control run was performed with zero electric field, which was accomplished by grounding the lower electrode at $t = 2$ ms. Thus, in that control run, particles were influenced by only two forces, gravity and gas drag. In the other two runs, we applied upward DC electric fields of 23.4 and 27.6 V cm^{-1} for lifting control. These upward fields were produced by applying DC potentials of +170 V and +200 V, respectively, starting at $t = 2$ ms.

A time sequence for the voltage on the lower electrode is sketched in figure 2. For $t < 0$, the 13 MHz RF power was on, with a peak-to-peak amplitude of 305 V. A self-bias voltage of -150 V developed on the lower electrode. At $t = 0$, the RF power was turned off.

For $0 < t < 2$, even though the RF power was turned off, the lower electrode retained its -150 V DC negative potential, due to the presence of coupling capacitor $C_{\rm coupl}$. It was during this time that the particle's charge became frozen. For $t > 2$ ms, a positive voltage $V_{\rm bias}$ was applied to the lower electrode using the transistor switch circuit, which overwhelmed the coupling capacitor that had been determining the DC bias until then. The value of $V_{\rm bias}$ was zero for the control run, and +170 and +200 V for the other runs reported here. The corresponding electric fields were 0, 23.4 and 27.6 V cm^{-1}.

3. Experimental results

In figure 3 we present results for particle height versus time for three runs. These include a control run with $E = 0$, and runs with an upward electric field $E = 23.4$ and 27.6 V cm^{-1}.

The run at $E = 27.6$ V cm^{-1} provided our most significant result: at that electric field, the upward lifting force was sufficient to prevent particles from falling to the lower electrode. Initially they fell downward during the first 2 ms, gaining a small downward initial velocity that was due to a combination of gravity and electric forces, which were both downward during this early period. Later, when the electric field was reversed at $t = 2$ ms, the downward fall of particles was arrested as they experienced a small upward net force.

We can estimate the net upward force in that run at $E = 27.6$ V cm^{-1} by fitting the time series for height in figure 3. This fitting was done in the time interval $30 \leqslant t \leqslant 70$ ms, when the velocity was low enough to neglect gas friction, so that we could simply fit to a parabola. This fit yielded an acceleration of 1.114 m s^{-2}, corresponding to a net upward force of 5.79×10^{-13} N. This net force was $F_{\rm lift}$–mg, where $g = 9.804$ m s^{-2} is the acceleration of gravity at the location of our lab [89]. This result allows us to calculate the upward lifting force $F_{\rm lift} = QE = 5.67\times10^{-12}$ N. We calculated the particle charge as $Q = +13\,000\,e$, during the late stage of the afterglow. This was done using equation (11) of [74],with inputs of acceleration, particle mass, and the electric field from solving Laplace's equation. The latter [74] assumes that electron and ion densities are negligible during the measurement interval, which we confirmed by measuring the voltage waveform

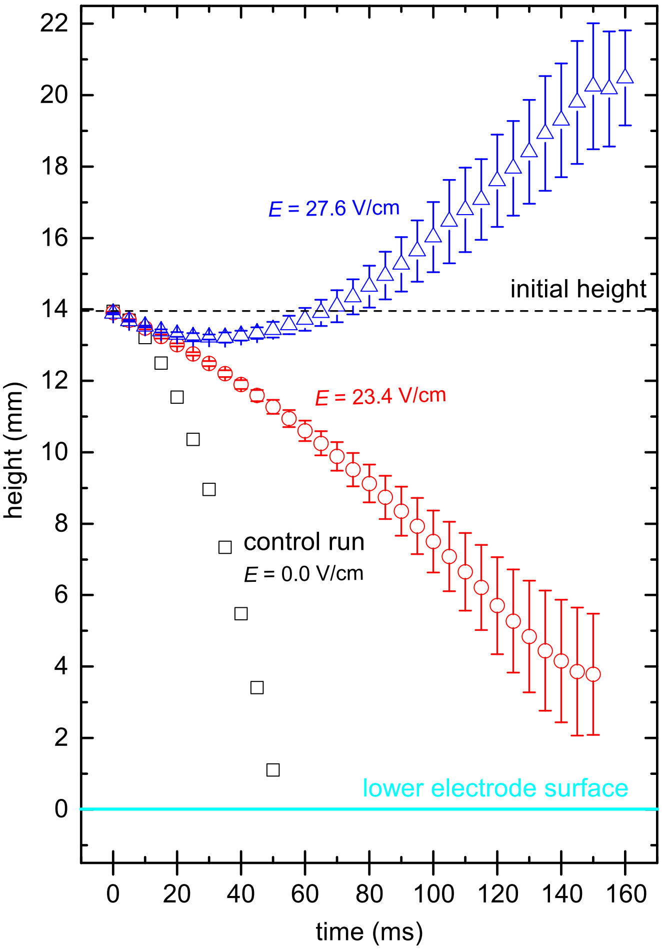

Figure 3. Dust particle height after turning the plasma off. The time series includes both the early stage of the afterglow when the particle charge was developing, and the late stage beginning when the particle charge was frozen, which was estimated in [77] to be 1.5 ms. Beginning after the delay $t = 2$ ms, the lifting force was applied, and it was sufficient in the run at $E = 27.6\ \mathrm{V\,cm^{-1}}$ to prevent the particles from falling to the lower electrode. In the run at a slightly weaker $E = 23.4\ \mathrm{V\,cm^{-1}}$, the particles fell, but much more slowly than in the control run with no electric field. The charge Q was the same in all runs, as it was determined during the early stage of the afterglow. Using the heights of about 40 particles, we calculated the each data point as the mean of those heights. Also shown are bars which indicate the standard deviation of the mean. (These bars are not intended to be error bars, i.e. they are not the standard deviation of the mean, which would be about six-fold smaller.) For the control run, the rms dispersion was smaller than the symbol size.

on the lower electrode (and thereby the current-collection waveform on the coupling capacitor) as in [74]. We note that the mass of these melamine-formaldehyde particles has been reported to diminish by up to 10% due to vacuum exposure [91, 92], if such a mass loss occurred in our experiment, our value for the charge may be an overestimate, by as much as 10%.

The gas friction force played a role in this experiment only at the highest velocities. For the run with $E = 27.6\ \mathrm{V\,cm^{-1}}$, we calculated that drag became about 20% of the total force when the particles reached a velocity of about $100\ \mathrm{mm\,s^{-1}}$. Such velocities were attained in that run for $t > 70$ ms, in the run at $E = 27.6\ \mathrm{V\,cm^{-1}}$.

In the other two runs ($E = 0$ and $E = 23.4\ \mathrm{V\,cm^{-1}}$), the particles were not forced upward sufficiently to prevent them from falling to the lower electrode. In the run at the slightly reduced electric field of $E = 23.4\ \mathrm{V\,cm^{-1}}$, the particles were pushed upward, but with not enough force to overcome gravity, so that they fell gently. In that run, the particles fell at a low velocity of about $150\ \mathrm{mm\,s^{-1}}$, with accelerations that did not exceed $1\ \mathrm{m\,s^{-2}}$.

In the control run with $E = 0$, the particles fell to the lower electrode much more rapidly than in the runs when we applied a lifting force. Even though the particles were charged, they experienced no electric force in the control run because the electric field was zero, due to grounding all chamber surfaces. The downward acceleration was initially $9.6\ \mathrm{m\,s^{-2}}$, which is only slightly different from that of gravity, presumably due to gas drag or measurement errors.

4. Conclusion

The plasma afterglow and its conditions are crucial in determining the outcome of how particles fall, or do not fall, and thereby contaminate surfaces at the end of a plasma processing step. Taking advantage of our recent advances in understanding the fundamental physics of particle charging in the afterglow, we have described a particle-mitigation scheme that controls two factors during the plasma afterglow: the particle charge and the particle lifting force. The particle charge is determined by conditions in the early stage of the afterglow, when electrons and ions remain in sufficient number to alter the particle's charge. The present paper mostly concerns the particle lifting force, during the late stage of the afterglow.

From the experiment reported here, we conclude that the falling of the charged particles can be slowed and even stopped altogether. This outcome, which is desirable for avoiding particle contamination of lower surfaces, is accomplished by applying a vertical electric field with a particular timing and magnitude.

We reported three experimental runs. In the control run, zero electric field was applied during the late stage of the afterglow, and the particles fell with an acceleration of nearly 1 g. We also performed two runs with an upward vertical electric field, which differed by <20% for the two runs. In the run with the larger electric field, the particles were actually lifted upward above their initial height. In the run with a slightly reduced electric field, the lifting force did not quite balance gravity, and the charged particles drifted slowly downward, reaching velocities of about $50\ \mathrm{mm\,s^{-1}}$.

To control the lifting force, for this paper we used a DC power supply and a transistor switch to apply a desired electric field, after the particle charge had become frozen. One could do more, and actually control both the charge and the lifting force, using two power supplies switched separately at different times. One power supply would be for controlling the lifting force during the late stage of the afterglow, as in the present experiment. The other power supply would be applied earlier for charging control, during the early stage of the afterglow, while electrons and ions are still present in significant numbers. For charging control, one can either apply a positive potential to the lower electrode to clear its vicinity of ions so that particles are charged negatively, or a negative potential to clear electrons away from the electrode's vicinity and drive ions through the particle cloud at a controlled energy, yielding a controlled positive charge.

We can envision using the controlled lifting method described here under conditions different from those of the present experiment. Two parameters would need to be adjusted according to the conditions: the electric field and the timing delay. We expect at least three factors would require such adjustments: particle size, gas pressure, and presence of negative ions. The particle size we used was large, 8.69 μm diameter, to allow imaging them individually as they fell. We expect that a weaker DC electric field could be sufficient to lift smaller particles, since the charge-to-mass ratio decreases with particle size. At higher gas pressures than 8 mTorr as in our experiment, gas drag can slow the transport of electrons and ions in the afterglow; we expect that this slower transport could delay the freezing of particle charges, and accordingly require a greater timing delay for applying the DC electric field for lifting. Similarly, the presence of negative ions (as is common in reactive plasmas) would alter the transport of electrons and ions, and possibly the magnitude of the particle charge as well, which would again require an adjustment of the electric field and its timing delay.

Data availability statement

All data that support the findings of this study are included within the article (and any supplementary files).

Acknowledgments

This work was supported by the Army Research Office under MURI Grant No. W911NF-18-1-0240, the United States Department of Energy under Grant No. DE-SC0014566 and NASA/JPL RSA Nos. 1672641 and 1689926, and the National Science Foundation under Grant No. PHY-1740379. We thank our MURI team for helpful discussions, and Steven J Lanham & Mark J Kushner for their numerical solution of Laplace's equation in our plasma chamber. This work is related to a pending patent, Serial Number PCT/US2023/03392, where Neeraj Chaubey and J Goree are co-inventors.

ORCID iD

Neeraj Chaubey https://orcid.org/0000-0003-1964-9152

References

[1] Bouchoule A 1999 *Dusty Plasmas: Physics, Chemistry and Technological Impacts in Plasma Processing* (Wiley)
[2] Selwyn G S, Singh J and Bennett R 1989 *J. Vac. Sci. Technol.* A **7** 2758–65
[3] Shukla P K and Mamun A A 2002 *Introduction to Dusty Plasma Physics* vol 44 (IOP Publishing)
[4] Fortov V E, Khrapak A G, Khrapak S A, Molotkov V I and Petrov O F 2004 *Phys.-Usp.* **47** 447–92
[5] Tsytovich V N, Morfill G E, Vladimirov S V and Thomas H M 2008 *Elementary Processes in Complex Plasmas* (Springer) pp 67–140
[6] Melzer A and Goree J 2008 *Fundamentals of Dusty Plasmas* (Wiley) ch 6
[7] Goertz C K 1989 *Rev. Geophys.* **27** 271–92
[8] Choudhary M 2021 *Eur. J. Phys.* **42** 053001
[9] Barkan A and Merlino R L 1995 *Phys. Plasmas* **2** 3261–5
[10] Antonova T, Khrapak S A, Pustylnik M Y, Rubin-Zuzic M, Thomas H M, Lipaev A M, Usachev A D, Molotkov V I and Thoma M H 2019 *Phys. Plasmas* **26** 113703
[11] Thomas E, Konopka U, Merlino R L and Rosenberg M 2016 *Phys. Plasmas* **23** 055701
[12] Merlino R L, Meyer J K, Avinash K and Sen A 2016 *Phys. Plasmas* **23** 064506
[13] Meyer J K and Merlino R L 2016 *IEEE Trans. Plasma Sci.* **44** 473–8
[14] Merlino R L, Meyer J K, Barkan A, Avinash K and Sen A 2018 *AIP Conf. Proc.* **1925** 020021
[15] Choudhary M, Bergert R, Mitic S and Thoma M H 2020 *Phys. Plasmas* **27** 063701
[16] Samsonov D, Goree J, Thomas H M and Morfill G E 2000 *Phys. Rev.* E **61** 5557–72
[17] Nunomura S, Samsonov D and Goree J 2000 *Phys. Rev. Lett.* **84** 5141–4
[18] Hebner G A, Riley M E and Greenberg K E 2002 *Phys. Rev.* E **66** 046407
[19] Nosenko V, Goree J, Ma Z W, Dubin D H E and Piel A 2003 *Phys. Rev.* E **68** 056409
[20] Hartmann P, Kalman G J, Donkó Z and Kutasi K 2005 *Phys. Rev.* E **72** 026409
[21] Feng Y, Goree J and Liu B 2007 *Rev. Sci. Instrum.* **78** 053704
[22] Knapek C A, Samsonov D, Zhdanov S, Konopka U and Morfill G E 2007 *Phys. Rev. Lett.* **98** 015004
[23] Ruhunusiri W D S, Goree J, Feng Y and Liu B 2011 *Phys. Rev.* E **83** 066402
[24] Singh Dharodi V, Kumar Tiwari S and Das A 2014 *Phys. Plasmas* **21** 073705
[25] Bose S, Kaur M, Chattopadhyay P, Ghosh J, Thomas E and Saxena Y 2019 *J. Plasma Phys.* **85** 905850110
[26] Tiwari S, Dharodi V, Das A, Kaw P and Sen A 2014 *J. Plasma Phys.* **80** 817–23
[27] Choudhary M, Mukherjee S and Bandyopadhyay P 2017 *Phys. Plasmas* **24** 033703
[28] Kostadinova E, Guyton F, Cameron A, Busse K, Liaw C, Matthews L and Hyde T 2018 *Contrib. Plasma Phys.* **58** 209–16
[29] Kananovich A and Goree J 2020 *Phys. Rev.* E **101** 043211
[30] Kaur M, Bose S, Chattopadhyay P, Sharma D, Ghosh J and Saxena Y 2015 *Phys. Plasmas* **22** 033703
[31] Kaur M, Bose S, Chattopadhyay P, Sharma D, Ghosh J, Saxena Y and Thomas J E 2015 *Phys. Plasmas* **22** 093702
[32] Dharodi V S 2020 *Phys. Rev.* E **102** 043216
[33] Choudhary M, Bergert R, Moritz S, Mitic S and Thoma M H 2021 *Contrib. Plasma Phys.* **61** e202000110
[34] Knapek C A, Couedel L, Dove A, Goree J, Konopka U, Melzer A, Ratynskaia S, Thoma M H and Thomas H M 2022 *Plasma Phys. Control. Fusion* **64** 124006

[35] Zhuravlyov V, Goree J, Douglas J F, Elvati P and Violi A 2022 *Phys. Rev.* E **106** 055212
[36] Zhuravlyov V, Goree J, Elvati P and Violi A 2023 *Phys. Rev.* E **108** 035211
[37] Selwyn G S 1994 *Plasma Sources Sci. Technol.* **3** 340
[38] Sikimić B, Stefanović I, Denysenko I B and Winter J 2013 *Plasma Sources Sci. Technol.* **22** 045009
[39] Sikimić B, Stefanović I, Denysenko I, Winter J and Sadeghi N 2014 *Plasma Sources Sci. Technol.* **23** 025010
[40] Stefanović I, Sadeghi N, Winter J and Sikimić B 2017 *Plasma Sources Sci. Technol.* **26** 065014
[41] Chen Y M, Sawadichai R, Tian S, Donnelly V M, Ruchhoeft P and Economou D J 2019 *J. Phys. D: Appl. Phys.* **52** 355205
[42] Platier B, Limpens R, Lassise A, Staps T, Van Ninhuijs M, Daamen K, Luiten O, IJzerman W and Beckers J 2020 *Appl. Phys. Lett.* **116** 103703
[43] Chen Z, Blakeney J, Carruth M, Ventzek P L and Ranjan A 2022 *J. Vac. Sci. Technol.* B **40** 033601
[44] Staps T, Platier B, Mihailova D, Meijaard P and Beckers J 2021 *Rev. Sci. Instrum.* **92** 093504
[45] Collins S, Brown D, O'Hanlon J and Carlile R 1996 *J. Vac. Sci. Technol.* A **14** 634–8
[46] Setyawan H, Shimada M, Imajo Y, Hayashi Y and Okuyama K 2003 *J. Aerosol Sci.* **34** 923–36
[47] Ivlev A V *et al* 2003 *Phys. Rev. Lett.* **90** 055003
[48] Couëdel L, Mikikian M, Boufendi L and Samarian A A 2006 *Phys. Rev.* E **74** 026403
[49] Couëdel L, Samarian A A, Mikikian M and Boufendi L 2008 *Phys. Plasmas* **15** 063705
[50] Couëdel L, Mezeghrane A, Samarian A, Mikikian M, Tessier Y, Cavarroc M and Boufendi L 2009 *Contrib. Plasma Phys.* **49** 235–59
[51] Schweigert I V and Alexandrov A L 2012 *J. Phys. D: Appl. Phys.* **45** 325201
[52] Saxena V, Avinash K and Sen A 2012 *Phys. Plasmas* **19** 093706
[53] Wörner L *et al* 2013 *Phys. Plasmas* **20** 123702
[54] Denysenko I B, Stefanović I, Sikimić B, Winter J and Azarenkov N A 2013 *Phys. Rev.* E **88** 023104
[55] Denysenko I B, Kersten H and Azarenkov N A 2016 *Phys. Plasmas* **23** 053704
[56] Denysenko I B, Azarenkov N A, Ostrikov K and Yu M Y 2018 *Phys. Plasmas* **25** 013703
[57] Piel A and Goree J A 2013 *Phys. Rev.* E **88** 063103
[58] Denysenko I B, Mikikian M and Azarenkov N A 2021 *J. Phys. D: Appl. Phys.* **55** 095201
[59] van Huijstee J C A, Blom P, Peijnenburg A T A and Beckers J 2022 *Front. Phys.* **10** 926160
[60] van Minderhout B, Peijnenburg T, Blom P, Vogels J M, Kroesen G M W and Beckers J 2019 *J. Phys. D: Appl. Phys.* **52** 32LT03
[61] van Minderhout B, van Huijstee J C A, Platier B, Peijnenburg T, Blom P, Kroesen G M W and Beckers J 2020 *Plasma Sources Sci. Technol.* **29** 065005
[62] Sharma G, Abuyazid N, Dhawan S, Kshirsagar S, Sankaran R M and Biswas P 2020 *J. Phys. D: Appl. Phys.* **53** 245204
[63] Suresh V, Li L, Felipe J R G and Gopalakrishnan R 2021 *J. Phys. D: Appl. Phys.* **54** 275205
[64] van Minderhout B, van Huijstee J C A, Peijnenburg A T A, Blom P, Kroesen G M W and Beckers J 2021 *Plasma Sources Sci. Technol.* **30** 045016
[65] Chaudhuri M, Couëdel L, Thomas J E, Huber P, Lipaev A M, Thomas H M and Schwabe M 2021 arXiv:2103.09607
[66] Denysenko I, Mikikian M and Azarenkov N 2022 *Phys. Plasmas* **29** 093702
[67] Couëdel L 2022 *Front. Phys.* **10** 1015603
[68] Staps T 2022 *Front. Phys* **10** 988812
[69] van Huijstee J C A, Blom P and Beckers J 2023 *Phys. Plasmas* **30** 033704
[70] Chaudhuri M, Heijmans L, van de Kerkhof M, Krainov P, Astakhov D and Yakunin A 2023 *Plasma Sources Sci. Technol.* **32** 095005
[71] Beckers J, van Huijstee J, Blom P, Medini F and Peijnenburg T 2023 The role of neutral drag force in pulsed plasma enabled particle contamination control *Proc. SPIE* **12496** 804–10
[72] Choudhary M 2023 *Contrib. Plasma Phys.* e202300072
[73] Kumar K, Bandyopadhyay P, Singh S, Dharodi V S and Sen A 2023 *Sci. Rep.* **13** 3979
[74] Chaubey N, Goree J, Lanham S J and Kushner M J 2021 *Phys. Plasmas* **28** 103702
[75] Chaubey N and Goree J 2022 *Front. Phys.* **10** 879092
[76] Chaubey N and Goree J 2022 *Phys. Plasmas* **29** 113705
[77] Chaubey N and Goree J 2023 *J. Phys. D: Appl. Phys.* **56** 375202
[78] Su Y J, Gupta A, Hills G W and Lanucha J 1995 Use of electrostatic forces to reduce particle contamination in semiconductor plasma processing chambers *US Patent* 5,410,122
[79] Lantsman A D 1996 Plasma processing system with reduced particle contamination *US Patent* 5,573,597
[80] Dornfest C, Gupta A and Girard G 1998 Method and apparatus for removing particulates from semiconductor substrates in plasma processing chambers *US Patent* 5,779,807
[81] Moriya T and Nagaike H 2010 Particle removal apparatus and method and plasma processing apparatus *US Patent* 7,651,586
[82] Moriya T and Nagaike H 2011 Particle removal apparatus and method and plasma processing apparatus *US Patent* 8,052,798
[83] Marion J, Yoshida Y, Bathrick B, Voronin S and Ranjan A 2018 Manufacturing methods to reduce surface particle impurities after a plasma process *US Patent App.* 15/969,472
[84] Dhas A, Boumatar K and Ramsayer C J 2018 Defect control and stability of DC bias in RF plasma-based substrate processing systems using molecular reactive purge gas *US Patent* 10,047,438
[85] Augustyniak E, Ramsayer C J, Singhal A N and Boumatar K 2018 Defect control in RF plasma substrate processing systems using DC bias voltage during movement of substrates *US Patent* 10,081,869
[86] Wohlfahrt S and Block D 2021 *Phys. Plasmas* **28** 123701
[87] Liu B, Goree J, Nosenko V and Boufendi L 2003 *Phys. Plasmas* **10** 9–20
[88] Schepers L, IJzerman W and Beckers J 2018 *J. Phys. D: Appl. Phys.* **51** 375203
[89] Pavlis N K, Holmes S A, Kenyon S C and Factor J K 2012 *J. Geophys. Res.* **117** B04406
[90] Rasband W S 1997–2018 computer code ImageJ (U. S. National Institutes of Health) (available at: https://imagej.nih.gov/ij/)
[91] Pavlu J, Velyhan A, Richterova I, Nemecek Z, Safrankova J, Cermak I and Zilavy P 2004 *IEEE Trans. Plasma Sci.* **32** 704–8
[92] Carstensen J, Haase F, Jung H, Tadsen B, Groth S, Greiner F and Piel A 2013 *IEEE Trans. Plasma Sci.* **41** 764–8
[93] Purchased from Microparticles GmbH (available at: www.microparticles.de)